



(Print)

Section A

(Online)



Estd. 1989

JOURNAL OF ULTRASCIENTIST OF PHYSICAL SCIENCES
 An International Open Free Access Peer Reviewed Research Journal of Mathematics
 website:- www.ultrascientist.org

MHD chemically reacting and radiating nanofluid flow over a vertical cone embedded in a porous medium with variable properties

S.R. RAVI CHANDRA BABU^{1,*}, S. VENKATESWARLU² and K. JAYA LAKSHMI³

^{1*}Research scholar, Dept of Mathematics, JNTUA, Anantapur, A.P, (India)

²Department of mathematics, RGM College of Engineering & Technology, Nandyal, A.P, (India)

³Department of mathematics, JNTUA, Anantapur, A.P, (India)

*Corresponding author Email: ravichandrababusr@gmail.com

<http://dx.doi.org/10.22147/jusps-A/300202>

Acceptance Date 21st December, 2017,

Online Publication Date 2nd February, 2018

Abstract

In this study, we examine the combined effects of thermal radiation, chemical reaction on MHD hydromagnetic boundary layer flow over a vertical cone filled with nanofluid saturated porous medium under variable properties. The governing flow, heat and mass transfer equations are transformed into ordinary differential equations using similarity variables and are solved numerically by a Galerkin Finite element method. Numerical results are obtained for dimensionless velocity, temperature, nanoparticle volume fraction. The effects of various controlling parameters on these quantities are investigated. Pertinent results are presented graphically and discussed quantitatively. The present results are compared with existing results and found to be good agreement. It is found that the temperature of the fluid remarkably enhances with the rising values of Brownian motion parameter (Nb).

Keywords: MHD; Nanofluid; Vertical cone; Variable properties; Chemical reaction; Thermal radiation.

1. Introduction

In recent years the field of science and technology, nanotechnology has become more popular because of its specific application to the arenas of electronics, fuel cells, space, fuels, better air quality, batteries, solar cells, medicine, cleaner water, chemical sensors and sporting goods. In the understanding of all these features, there is a vital field acknowledged as the nanofluid, which is fundamentally a homogenous mixture of the base fluid and nanoparticles. Nanoparticles are the particles and are of 1-100 nm in size. The convective heat transfer fluids like water, oil, kerosene and ethylene glycol have poor heat transfer capabilities due to their low

thermal conductivity. To improve the thermal conductivity of these fluids nano/micro-sized materials are suspended in liquids. The thermal conductivity of the metals is three times higher than the general fluids, so it is desirable to combine the two substances. Due to the nanofluid thermal enhancement, performance, applications and benefits in several important arenas, the nanofluid has contributed significantly well in the field of microfluidics, manufacturing, microelectronics, advanced nuclear systems, polymer technology, transportation, medical, saving in energy. Choi¹ was the first among all who introduced a new type of fluid called nanofluid while doing research on new coolants and cooling technologies. Eastman *et al.*² have noticed in an experiment that the thermal conductivity of the base fluid (water) has increased up to 60% when CuO nanoparticles of volume fraction 5% are added to the base fluid. This is because of increasing surface area of the base fluid due to the suspension of nanoparticles. Eastman *et al.*³ have also showed that the thermal conductivity has increased 40% when copper nanoparticles of volume fraction less than 1% are added to the ethylene glycol or oil. Xuan *et al.*⁴ have reported that the convective flow and heat transfer characteristics of nanofluids. Buongiorno⁵ has reported in experimental study that nanoparticle size, inertia, particle agglomeration, Magnus effect, volume fraction of the nanoparticle, Brownian motion and thermophoresis are the influencing parameters. Nield and Kuznetsov⁶ have discussed the Cheng-Mincowycz problem for natural convection boundary-layer flow in a porous medium saturated nanofluid. Kuznetsov and Nield⁷ studied the influence of Brownian motion and thermophoresis on natural convection boundary layer flow of a nanofluid past a vertical plate.

Chamkha *et al.*⁸ analyzed the sway of thermo-diffusion and Diffusion-thermo effects on mixed convection flow of nanofluid over a vertical cone saturated in a porous medium with chemical reaction. Chamkha *et al.*⁹ have discussed the mixed convection flow of nanofluid over vertical cone embedded in porous medium with thermal radiation. Gorla *et al.*¹⁰ have studied nanofluid natural convection boundary layer flow through porous medium over a vertical cone. Chamkha *et al.*¹¹ have investigated Non-Newtonian nanofluid natural convection flow over a cone through porous medium with uniform heat and volume fraction fluxes. Sudarsana Reddy *et al.*¹² have presented natural convection boundary layer heat and mass transfer characteristics of Al₂O₃ - water and Ag - water nanofluids over a vertical cone. In all the above studies the viscosity and thermal conductivity of nanofluids are taken as constant. Sudarsana Reddy *et al.*¹³ have discussed the effect of variable viscosity and thermal conductivity on heat and mass transfer flow of nanofluid over a stretching sheet. Sudarsana Reddy¹⁴ has discussed MHD natural convection heat transfer enhancement of Cu – water and Ag – water based nanofluid over a rotating disk under the influence of chemical reaction.. In this study they have considered three types of nanoparticles, Al₂O₃, TiO₂ and CuO with ethylene vinyl acetate copolymer (EVA) as the base fluid and reported that CuO – EVA based nanofluid has better heat transfer enhancement than the Al₂O₃ – EVA and TiO₂ – EVA nanofluid. Raghunath and Siva Prasad¹⁷ discussed heat and mass transfer on unsteady MHD flow of a visco elastic fluid past an infinite vertical oscillating porous plate.

The main aim of this article is to address the influence of variable viscosity and variable thermal conductivity on MHD boundary layer heat and mass transfer flow of nanofluid over a vertical cone embedded in porous medium with thermal radiation and chemical reaction. As a result the parameters (Nv) and (Nc) are entered into the problem. The problem presented here has immediate applications in biomedical systems, electronic devices, food processing, manufacturing, cooling systems, etc. To our knowledge, the problem is new and no such articles reported yet in the literature.

2. Mathematical Analysis of the Problem :

We assume a steady two-dimensional viscous incompressible natural convection nanofluid flow over a vertical cone embedded in porous medium in the presence of variable viscosity and thermal conductivity with the coordinate system given in Fig.1. The fluid is assumed an electrically conducted through a non-uniform

magnetic field of strength B_0 applied in the direction normal to the surface of the cone. It is assumed that T_w , and ϕ_w are the temperature and nanoparticle volume fraction at the surface of the cone ($y=0$) and T_∞ and ϕ_∞ are the temperature and nanoparticle volume fraction of the ambient fluid, respectively. Based on the works of Buongiorno⁵ and by employing the Oberbeck - Boussinesq approximation the governing equations describing the flow, heat and mass transfer for nanofluids in the presence of thermal radiation and chemical reaction parameters take the following form:

$$\frac{\partial(ru)}{\partial x} + \frac{\partial(rv)}{\partial y} = 0 \quad (1)$$

$$\frac{\partial p}{\partial y} = 0 \quad (2)$$

$$\frac{\partial p}{\partial x} = -\frac{\mu(T)}{K}u + g[(1 - \phi_\infty)\rho_{f\infty}\beta(T - T_\infty) - (\rho_p - \rho_{f\infty})(\phi - \phi_\infty)]\cos\gamma - \frac{\sigma\beta_0^2}{\rho_f}u \quad (3)$$

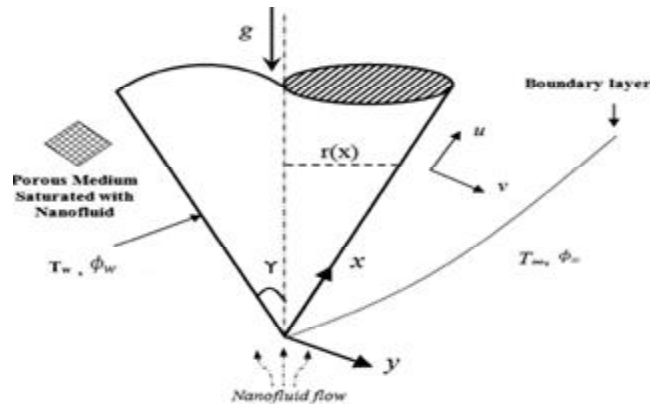


Fig.1. Physical model and coordinate system

$$\left(u \frac{\partial T}{\partial x} + v \frac{\partial T}{\partial y}\right) = \frac{1}{(\rho c_p)_{nf}} \frac{\partial}{\partial y} \left(k_m(T) \frac{\partial T}{\partial y} \right) + \frac{(\rho c)_p}{(\rho c_p)_{nf}} \left[D_B \frac{\partial \phi}{\partial y} \cdot \frac{\partial T}{\partial y} + \left(\frac{D_T}{T_\infty} \right) \left(\frac{\partial T}{\partial y} \right)^2 \right] - \frac{1}{(\rho c_p)_{nf}} \cdot \frac{\partial}{\partial y} (q_r) \quad (4)$$

$$\frac{1}{\varepsilon} \left(u \frac{\partial \phi}{\partial x} + v \frac{\partial \phi}{\partial y} \right) = D_B \frac{\partial^2 \phi}{\partial y^2} + \left(\frac{D_T}{T_\infty} \right) \frac{\partial^2 T}{\partial y^2} - K_r (\phi - \phi_\infty) \quad (5)$$

The corresponding boundary conditions are

$$u = 0, \quad T = T_w, \quad \phi = \phi_w \quad \text{at} \quad y = 0 \quad (6)$$

$$u \rightarrow 0, \quad T \rightarrow T_\infty, \quad \phi \rightarrow \phi_\infty \quad \text{at} \quad y \rightarrow \infty \quad (7)$$

In the present study, the thermal conductivity and viscosity are taken as the function of temperature. Therefore, the viscosity in terms of temperature can be written as follows:

$$\frac{1}{\mu} = \frac{1}{\mu_\infty} [1 + \gamma(T - T_\infty)] \quad (8)$$

The above equation can be simplified as

$$\frac{1}{\mu} = m_{\mu}(T - T_r) \quad (9)$$

where, m_{μ} and T_r are can be defined as

$$m_{\mu} = \frac{\gamma}{\mu_{\infty}} \quad \text{and} \quad T_r = T_{\infty} - \frac{1}{\gamma}.$$

In the above equations (8) and (9), μ_{∞} , m_{μ} , T_{∞} , T_r , and γ are constant values.

The thermal conductivity of nanoparticles is defined as

$$k_m(T) = k_{\infty}(1 + m_k(T - T_{\infty})) \quad (10)$$

where, $m_k = \frac{Nc}{(T_w - T_{\infty})}$ and Nc is the variable thermal conductivity parameter, k_{∞} is the effective thermal conductivity. By using Rosseland approximation for radiation, the radiative heat flux q_r is defined as

$$q_r = -\frac{4\sigma^*}{3K^*} \frac{\partial T^4}{\partial y} \quad (11)$$

where, σ^* is the Stephan-Boltzman constant, K^* is the mean absorption coefficient. We assume that the temperature differences within the flow are such that the term T^4 may be expressed as a linear function of temperature. This is accomplished by expanding T^4 in a Taylor series about the free stream temperature T_{∞} as follows:

$$T^4 = T_{\infty}^4 + 4T_{\infty}^3(T - T_{\infty}) + 6T_{\infty}^2(T - T_{\infty})^2 + \dots \quad (12)$$

Neglecting higher-order terms in the above equation (12) beyond the first degree in $(T - T_{\infty})$, we get

$$T^4 \cong 4T_{\infty}^3 T - 3T_{\infty}^4. \quad (13)$$

Thus, substituting Eq. (13) into Eq. (11), we get

$$q_r = -\frac{16T_{\infty}^3 \sigma^*}{3K^*} \frac{\partial T}{\partial y}. \quad (14)$$

The continuity equation (1) is satisfied by introducing a stream function (ψ) as

$$u = \frac{1}{r} \frac{\partial \psi}{\partial y}, \quad v = -\frac{1}{r} \frac{\partial \psi}{\partial x} \quad (15)$$

The following similarity transformations are introduced to simplify the mathematical analysis of the problem

$$\eta = \frac{y}{x} Ra_x^{1/2}, \quad f(\eta) = \frac{\psi}{\alpha_m r Ra_x^{1/2}}, \quad \theta(\eta) = \frac{T - T_{\infty}}{T_w - T_{\infty}}, \quad \phi(\eta) = \frac{\phi - \phi_{\infty}}{\phi_w - \phi_{\infty}}, \quad Nv = \frac{T_r - T_{\infty}}{T_w - T_{\infty}}, \quad (16)$$

where Ra_x is the local Rayleigh number and is defined as

$$Ra_x = \frac{g\beta K \rho_{f\infty}(1 - \phi_{\infty})(T_w - T_{\infty}) x \cos \gamma}{\mu_{\infty} \alpha_m} \quad (17)$$

and r coordinate is related to the x coordinate by $r = x \sin \gamma$. Using the similarity variables (16) and making use of Eqs. (14), the governing equations (3) - (5) together with boundary conditions (6) and (7) reduce to

$$\frac{Nv}{(Nv-\phi)} f'' + \frac{Nv}{(Nv-\phi)^2} f' \phi' - (\theta' - Nr \phi') - Mf' = 0, \quad (18)$$

$$(1 + R)\theta'' + Nc \phi \theta'' + \frac{3}{2} f \theta' + Nc \theta' \phi' + Nt(\theta')^2 + Nb \phi' \theta' = 0, \quad (19)$$

$$\phi'' + \frac{3}{2} Le f \phi' + \frac{Nt}{Nb} \theta'' - C1 \phi = 0. \quad (20)$$

The transformed boundary conditions are

$$\begin{aligned} \eta = 0, \quad f = 0, \quad \theta = 1, \quad \phi = 1, \\ \eta \rightarrow \infty, \quad f' = 0, \quad \theta = 0, \quad \phi = 0, \end{aligned} \quad (21)$$

where prime denotes differentiation with respect to η , and the key thermophysical parameters dictating the flow dynamics are defined by

$$\begin{aligned} Nr &= \frac{(\rho_p - \rho_{f\infty})(\phi_w - \phi_{\infty})}{\rho_{f\infty} \beta (T_w - T_{\infty})(1 - \phi_{\infty})}, \quad Nb = \frac{\varepsilon \beta (\rho c)_p D_B (\phi_w - \phi_{\infty})}{(\rho c)_f \alpha_m}, \quad Nt = \frac{\varepsilon (\rho c)_p D_T (T_w - T_{\infty})}{(\rho c)_f \alpha_m T_{\infty}}, \quad Le = \frac{\alpha_m}{\varepsilon D_B}, \\ Nv &= -\frac{1}{\gamma(\phi_w - \phi_{\infty})}, \quad M = \frac{\sigma \beta_0^2 x}{\rho Ra_x^{1/2}}, \quad R = \frac{16 T_{\infty}^3 \sigma^*}{3 K^* k}, \quad Cr = \frac{k_0 x^2}{D_B Ra_x}. \end{aligned}$$

Other quantities of practical interest in this problem are local Nusselt number (Nu_x) and the local Sherwood number (Sh_x), which are defined as

$$Nu_x = \frac{x q_w}{k_m (T_w - T_{\infty})}, \quad Sh_x = \frac{x J_w}{D_B (\phi_w - \phi_{\infty})}, \quad (22)$$

where, q_w is the wall heat flux and J_w is the wall mass flux. The set of ordinary differential equations (18) – (20) are highly non-linear, and therefore cannot be solved analytically. The finite-element method [36, 37, 38, 39] has been implemented to solve these non-linear equations.

3.1 Numerical procedure :

The Finite-element method (FEM) is such a powerful method for solving ordinary differential equations and partial differential equations. The basic idea of this method is dividing the whole domain into smaller elements of finite dimensions called finite elements. This method is such a good numerical method in modern engineering analysis, and it can be applied for solving integral equations including heat transfer, fluid mechanics, chemical processing, electrical systems, and many other fields. The procedure involved in the Finite-element method is as follows.

3.2 Variational formulation :

The variational form related with Eqs. (18) to (20) over a typical linear element (η_e, η_{e+1}) is given by

$$\int_{\eta_e}^{\eta_{e+1}} w_1 \left(\frac{Nv}{(Nv-\phi)} f'' + \frac{Nv}{(Nv-\phi)^2} f' \phi' - (\theta' - Nr \phi') - Mf' \right) d\eta = 0 \quad (23)$$

$$\int_{\eta_e}^{\eta_{e+1}} w_2 \left((1 + R)\theta'' + Nc \phi \theta'' + \frac{3}{2} f \theta' + Nc \theta' \phi' + Nt(\theta')^2 + Nb \phi' \theta' \right) d\eta = 0 \quad (24)$$

$$\int_{\eta_e}^{\eta_{e+1}} w_3 \left(\phi'' + \frac{3}{2} Le f \phi' + \frac{Nt}{Nb} \theta'' - C1 \phi \right) d\eta = 0 \quad (25)$$

where w_1 , w_2 , and w_3 are weighted functions and may be regarded as the variations in f , θ , and ϕ , respectively.

3.3 Finite- element formulation :

The finite-element form may be attained from above equations by replacing finite-element approximations of the form

$$f = \sum_{j=1}^3 f_j \psi_j, \quad \theta = \sum_{j=1}^3 \theta_j \psi_j, \quad \phi = \sum_{j=1}^3 \phi_j \psi_j \quad (26)$$

$$\text{with } w_1 = w_2 = w_3 = \psi_i, \quad (i = 1, 2, 3).$$

where ψ_i are the shape functions for a typical element (η_e, η_{e+1}) and are defined as

$$\psi_1^e = \frac{(\eta_{e+1} + \eta_e - 2\eta)(\eta_{e+1} - \eta)}{(\eta_{e+1} - \eta)^2}, \quad \psi_2^e = \frac{4(\eta - \eta_e)(\eta_{e+1} - \eta)}{(\eta_{e+1} - \eta)^2}, \quad \psi_3^e = \frac{(\eta_{e+1} + \eta_e - 2\eta)(\eta - \eta_e)}{(\eta_{e+1} - \eta)^2}, \quad \eta_e \leq \eta \leq \eta_{e+1} \quad (27)$$

The finite element model of the equations thus formed is given by

$$\begin{bmatrix} [K^{11}] & [K^{12}] & [K^{13}] \\ [K^{21}] & [K^{22}] & [K^{23}] \\ [K^{31}] & [K^{32}] & [K^{33}] \end{bmatrix} \begin{bmatrix} f \\ \theta \\ \phi \end{bmatrix} = \begin{bmatrix} \{r^1\} \\ \{r^2\} \\ \{r^3\} \end{bmatrix}$$

where $[K^{mn}]$ and $[r^m]$ ($m, n = 1, 2, 3$) are defined as

$$K_{ij}^{11} = -\frac{Nv}{(Nv-\phi)} \int_{\eta_e}^{\eta_{e+1}} \frac{\partial \psi_i}{\partial \eta} \frac{\partial \psi_j}{\partial \eta} d\eta + \frac{Nv}{(Nv-\phi)^2} \bar{f}_1 \int_{\eta_e}^{\eta_{e+1}} \psi_i \psi_1 \frac{\partial \psi_j}{\partial \eta} d\eta + \frac{Nv}{(Nv-\phi)^2} \bar{f}_2 \int_{\eta_e}^{\eta_{e+1}} \psi_i \psi_2 \frac{\partial \psi_j}{\partial \eta} d\eta - M \int_{\eta_e}^{\eta_{e+1}} \psi_i \frac{\partial \psi_j}{\partial \eta} d\eta,$$

$$K_{ij}^{12} = \int_{\eta_e}^{\eta_{e+1}} \psi_i \frac{\partial \psi_j}{\partial \eta} d\eta, \quad K_{ij}^{13} = -Nr \int_{\eta_e}^{\eta_{e+1}} \psi_i \frac{\partial \psi_j}{\partial \eta} d\eta, \quad K_{ij}^{21} = 0,$$

$$K_{ij}^{22} = (1 + R) \int_{\eta_e}^{\eta_{e+1}} \frac{\partial \psi_i}{\partial \eta} \frac{\partial \psi_j}{\partial \eta} d\eta + \frac{3}{2} \bar{f}_1 \int_{\eta_e}^{\eta_{e+1}} \psi_i \psi_1 \frac{\partial \psi_j}{\partial \eta} d\eta + \frac{3}{2} \bar{f}_2 \int_{\eta_e}^{\eta_{e+1}} \psi_i \psi_2 \frac{\partial \psi_j}{\partial \eta} d\eta +$$

$$Nt \int_{\eta_e}^{\eta_{e+1}} \psi_i \left(\frac{\partial \psi_j}{\partial \eta} \right)^2 d\eta + Nc \bar{\phi}_1 \int_{\eta_e}^{\eta_{e+1}} \psi_i \psi_1 \frac{\partial \psi_j}{\partial \eta} d\eta + Nc \bar{\phi}_2 \int_{\eta_e}^{\eta_{e+1}} \psi_i \psi_2 \frac{\partial \psi_j}{\partial \eta} d\eta,$$

$$K_{ij}^{23} = (Nc + Nb) \bar{\theta}_1 \int_{\eta_e}^{\eta_{e+1}} \psi_i \psi_1 \frac{\partial \psi_j}{\partial \eta} d\eta + (Nc + Nb) \bar{\theta}_2 \int_{\eta_e}^{\eta_{e+1}} \psi_i \psi_2 \frac{\partial \psi_j}{\partial \eta} d\eta,$$

$$K_{ij}^{31} = 0, \quad K_{ij}^{32} = \frac{Nt}{Nb} \int_{\eta_e}^{\eta_{e+1}} \frac{\partial \psi_i}{\partial \eta} \frac{\partial \psi_j}{\partial \eta} d\eta,$$

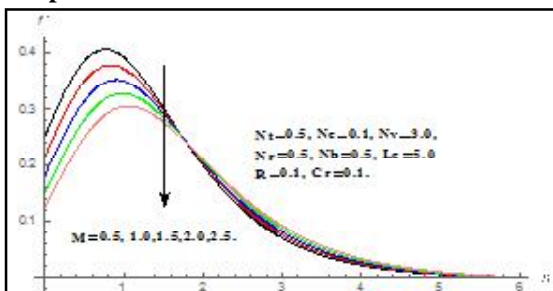
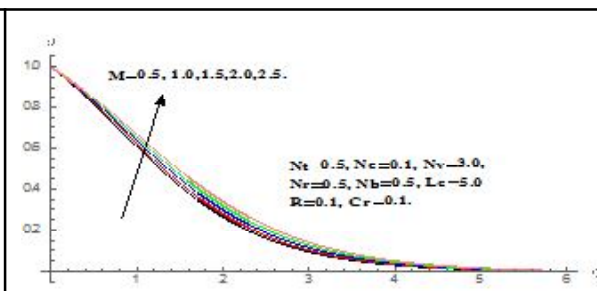
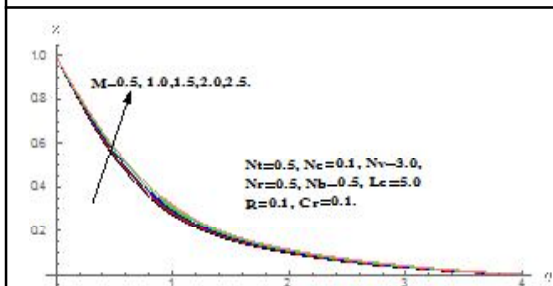
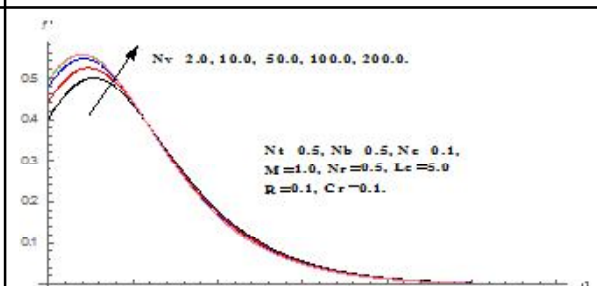
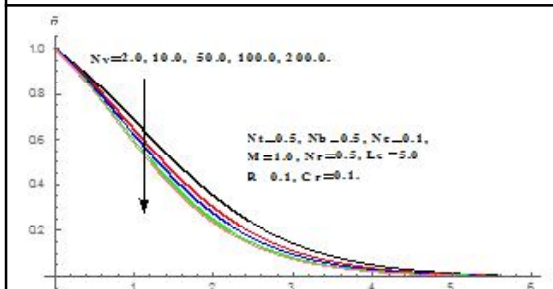
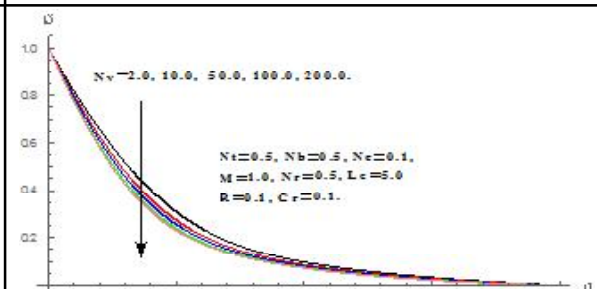
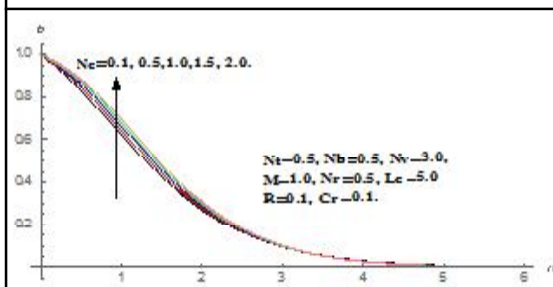
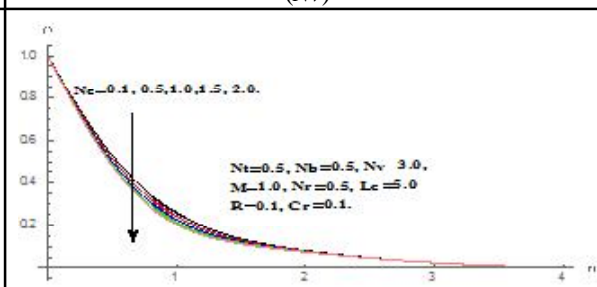
$$K_{ij}^{33} = \int_{\eta_e}^{\eta_{e+1}} \frac{\partial \psi_i}{\partial \eta} \frac{\partial \psi_j}{\partial \eta} d\eta + \frac{3}{2} Le \bar{f}_1 \int_{\eta_e}^{\eta_{e+1}} \psi_i \psi_1 \frac{\partial \psi_j}{\partial \eta} d\eta + \frac{3}{2} Le \bar{f}_2 \int_{\eta_e}^{\eta_{e+1}} \psi_i \psi_2 \frac{\partial \psi_j}{\partial \eta} d\eta - C1 \int_{\eta_e}^{\eta_{e+1}} \psi_i \psi_j d\eta,$$

$$r_i^1 = 0, \quad r_i^2 = -\left(\psi_i \frac{d\psi_i}{d\eta} \right)_{\eta_e}^{\eta_{e+1}}, \quad r_i^3 = -\left(\psi_i \frac{d\theta}{d\eta} + \frac{d\phi}{d\eta} \right)_{\eta_e}^{\eta_{e+1}}.$$

$$\text{where, } \bar{f} = \sum_{j=1}^3 f_j \frac{\partial \psi_i}{\partial \eta}, \quad \bar{\theta} = \sum_{j=1}^3 \theta_j \frac{\partial \psi_i}{\partial \eta}, \quad \bar{\phi} = \sum_{j=1}^3 \phi_j \frac{\partial \psi_i}{\partial \eta}.$$

After assembly of element equations, we get the system of strongly non-linear equations and are solved using a robust iterative scheme and are solved using Gauss elimination method.

Graphs:

Fig.2. Velocity profiles for various values of (M)Fig. 3. Temperature profiles for various values of (M)Fig. 4. Concentration profiles for various values of (M)Fig. 5. Velocity profiles for various values of (N_v)Fig. 6. Temperature profiles for various values of (N_v)Fig. 7. Concentration profiles for various values of (N_v)Fig. 8. Temperature profiles for various values of (N_c)Fig. 9. Concentration profiles for various values of (N_c)

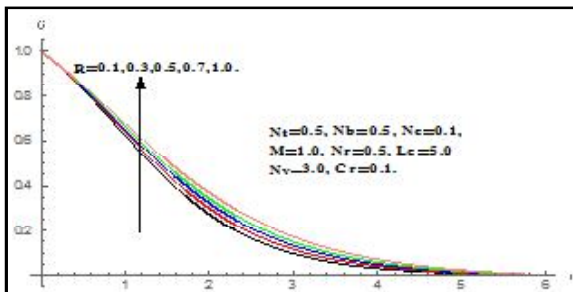


Fig.10. Temperature profiles for various values of (R)

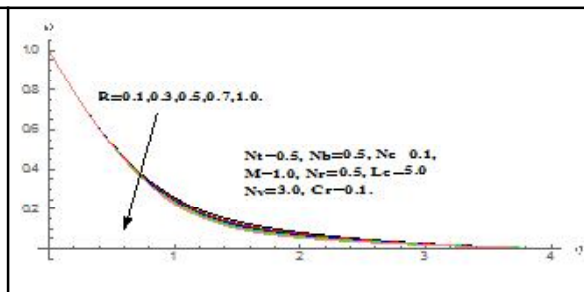


Fig.11. Concentration profiles for various values of (R)

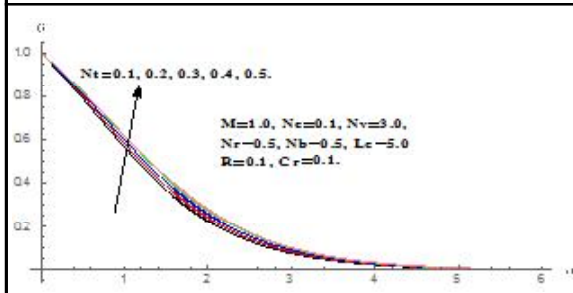


Fig.12. Temperature profiles for various values of (N_t)

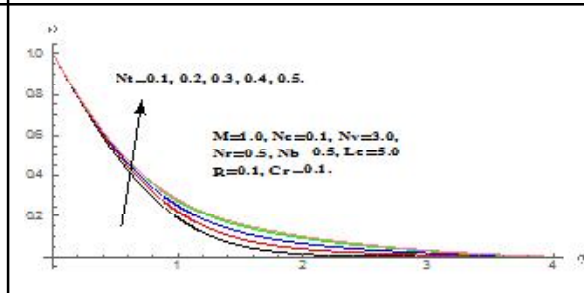


Fig.13. Concentration profiles for various values of (N_t)

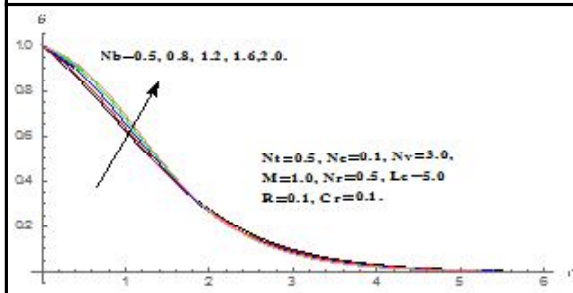


Fig. 14. Temperature profiles for various values of (N_b)

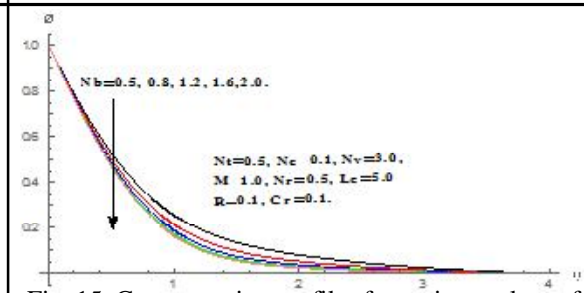


Fig. 15. Concentration profiles for various values of (N_b)

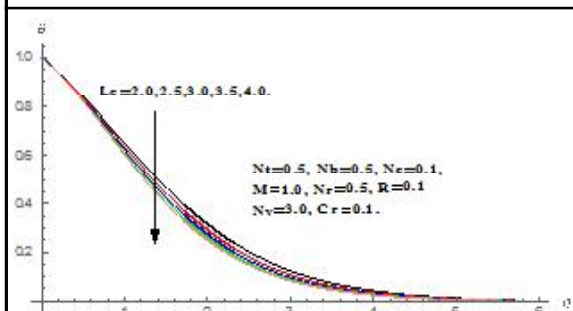


Fig. 16. Temperature profiles for various values of (Le)

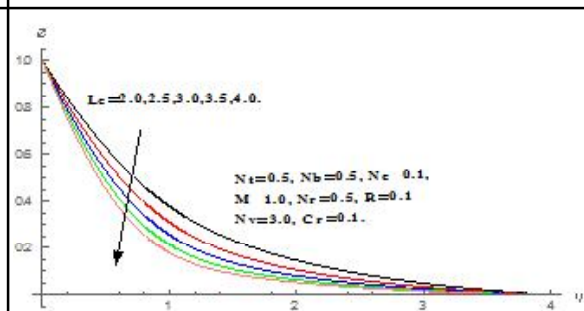


Fig. 17. Concentration profiles for various values of (Le)

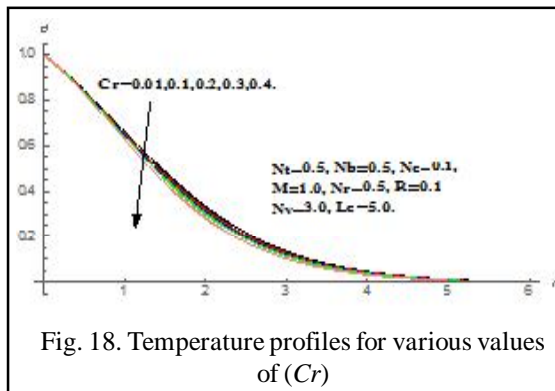


Fig. 18. Temperature profiles for various values of (Cr)

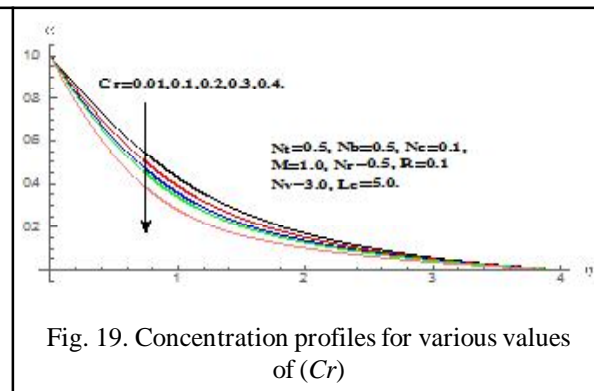


Fig. 19. Concentration profiles for various values of (Cr)

4. Results and Discussion

Computational results depicting the effects of various thermophysical parameters on the nanofluid velocity, temperature, nanoparticle volume fraction, The impact of magnetic parameter (M) on velocity (f'), temperature (θ) and concentration of nanoparticle (ϕ) profiles are illustrated in Figs. 2 – 4. It is observed that, the velocity profiles decelerate, whereas, temperature distributions heighten in the boundary layer regime with increment in magnetic parameter (M). As the values of magnetic parameter (M) rises, the thickness of the solutal boundary layer elevates in the fluid region (Fig. 4).

The velocity, temperature and nanoparticle volume fraction profiles for different values of variable viscosity parameter (Nv) are plotted in Figs. 5 – 7. It is clearly noticed from Fig. 5 that the velocity profiles are highly influenced by the variable viscosity parameter (Nv) in the vicinity of the cone surface. But, in the areas far away from the cone surface, inside the boundary layer, the velocity profiles are poorly affected by (Nv).

Figs. 8 and 9 illustrate the influence of variable thermal conductivity parameter (Nc) on thermal and solutal boundary layers. An increase in the values of variable thermal conductivity parameter (Nc) elevates the magnitude of temperature distributions (Fig. 8). This is because of the fact that the thermal conductivity raises near surface of the cone as the values of variable thermal conductivity parameter (Nc) increases. However, the thickness of the solutal boundary layer decelerates near the cone surface with the improving values of (Nc).

The non-dimensional profiles of temperature and concentration of nanoparticles are displayed in Figs. 10 and 11 for various values of radiation parameter (R). With the higher values of (R) the temperature of the fluid rises in the boundary layer regime. This is because of the fact that imposing thermal radiation into the flow warms the fluid, which causes an increment in the thickness of thermal boundary layer in the entire flow region (Fig.10). However, the concentration boundary layer thickness is deteriorated with increasing values of R .

Figures 12 and 13 depict the temperature (θ) and concentration (ϕ) distributions for various values of thermophoretic parameter (Nt). Both the temperature and concentration profiles elevate in the boundary layer region for the higher values of thermophoretic parameter (Nt)

Figures 14 – 15 shows the influence of Brownian motion parameter (Nb) on thermal and solutal boundary layer thickness. Brownian motion is the arbitrary motion of suspended nanoparticles in the base fluid and is more influenced by its fast moving atoms or molecules in the base fluid. It is worth to mention that Brownian motion is related to the size of nanoparticles and are often in the form of agglomerates and/or aggregates.

The influence of Lewis number (Le) on temperature and concentration evolutions is plotted in Figs. 16 and 17. It is observed that both the temperature and concentration distributions decelerate with the increasing values of the Lewis number in the entire boundary layer region.

The temperature and concentration profiles are depicted in Figs. 18 – 19 for diverse values of chemical

reaction parameter (Cr). It is noticed from Fig.18 that the temperature profiles of the fluid decelerated in the entire boundary layer regime with the higher values of chemical reaction parameter (Cr). The concentration profiles are highly influenced by the chemical reaction parameter. Chemical reaction parameter (Cr) increases means lesser the molecular diffusivity, as the result thinner the solutal boundary layer thickness (Fig. 19).

5. Conclusions

MHD natural convection boundary layer flow, heat and mass transfer characteristics over a vertical cone embedded in a porous medium saturated by a nanofluid under the impact of variable viscosity, variable thermal conductivity, thermal radiation and chemical reaction is investigated in this research. The important findings of the present study are summarized as follows.

- i) The velocity and temperature distributions are heightens whereas the nanoparticle volume fraction concentration profiles decelerate in the boundary layer region as the values of variable viscosity parameter (Nv) increases.
- ii) Increasing values of (Nc) elevates the thickness of thermal boundary layer. However, solutal boundary layer thickness deteriorates with the rising values of (Nc).
- iii) Increasing the values of variable viscosity parameter (Nv) raises the dimensionless rates of heat and mass transfer.
- iv) As the values of variable thermal conductivity parameter (Nc) increases the local Nusselt number values decreases whereas the values of local Sherwood number escalates in the fluid region.
- v) Both the temperature and concentration profiles elevates in the boundary layer regime as the values of (Nt) increases.
- vi) With increase in the values (Nb) upsurges the temperature of the fluid, however, it deteriorates the volume fraction concentration of nanoparticles.
- vii) Increase of chemical reaction parameter (Cr) depreciates the thickness of the solutal boundary layer.

6. References

1. Choi SUS. Enhancing thermal conductivity of fluids with nanoparticles, developments and applications of non-Newtonian flows, in: D.A. Siginer, H.P. Wang (Eds.), FED-Vol. 231/MD, Vol. 66, The American Society of Mechanical Engineers 99–105 (1995).
2. Eastman JA, Choi SUS, Li S, Thompson LJ, Lee S. Enhanced thermal conductivity through the development of nanofluid, in: S. Komarneni, J.C. Parker, H.J. Wollenberger (Eds.), Nanophase and Nanocomposite Materials II, MRS, Pittsburg, PA 3–11 (1997).
3. Eastman JA, Choi SUS, Li S, Yu W, Thompson LJ. Anomalously increased effective thermal conductivities of ethylene glycol-based nano-fluids containing copper nano-particles. *Appl. Phys. Lett.* 78, 718–720 (2001).
4. Xuan Y, Li Q, Investigation on Convective Heat Transfer and Flow Features of Nanofluids, *ASME J. Heat Transfer*, 125, 151–155 (2003).
5. Buongiorno J. Convective transport in nanofluids. *ASME J. Heat Transfer* 128, 240–250 (2006).
6. Nield DA, Kuznetsov AV, The Cheng - Minkowycz problem for natural convection boundary-layer flow in a porous medium saturated by a nanofluid. *Int. J. Heat Mass Transfer* 52, 5792–5795 (2009).
7. Kuznetsov AV, Nield DA, Natural convection boundary-layer of a nanofluid past a vertical plate. *Int. J. Therm. Sci* 49, 243–247 (2010).
8. Chamkha. A.J., Rashad. A.M, Unsteady Heat and Mass Transfer by MHD Mixed Convection Flow from a Rotating Vertical Cone with Chemical Reaction and Soret and Dufour Effects. *The Canadian Journal of Chemical Engineering* 92, 758-767 (2014).

9. Chamkha. A.J, Abbasbandy. S, Rashad. A. M, Vajravelu. K, Radiation effects on mixed convection about a cone embedded in a porous medium filled with a nanofluid, *Meccanica* 48, 275-285 (2013).
10. Gorla. R.S.R, Chamkha. A.J, Ghodeswar. V, Natural convective boundary layer flow over a vertical cone embedded in a porous medium saturated with a nanofluid, *Journal of Nanofluids* 3, 65-71 (2014).
11. Chamkha. A. J, Abbasbandy. S, Rashad. A. M, Non-Darcy natural convection flow of non-Newtonian nanofluid over a cone saturated in a porous medium with uniform heat and volume fraction fluxes, *International Journal of Numerical Methods for Heat and Fluid Flow* 25, 422-437 (2015).
12. Sudarsana Reddy. P, Suryanarayana Rao. K. V, MHD natural convection heat and mass transfer of Al_2O_3 - water and Ag - water nanofluids over a vertical cone with chemical reaction, *Procedia Engineering* 127, 476 – 484 (2015).
13. P. Sudarsana Reddy, Ali J. Chamkha, Influence of size, shape, type of nanoparticles, type and temperature of the base fluid on natural convection MHD of nanofluids, *Alexandria Eng. J.*, 55, 331-341 (2016).
14. P. Sudarsana Reddy, P. Sreedevi, Ali J. Chamkha, MHD boundary layer flow, heat and mass transfer analysis over a rotating disk through porous medium saturated by Cu-water and Ag-water nanofluid with chemical reaction, *Powder Technology* 307, 46 – 55 (2017).
15. Sudarsana Reddy, P and Chamkha, AJ, Soret and Dufour effects on MHD heat and mass transfer flow of a micropolar fluid with thermophoresis particle deposition, *Journal of Naval Architecture and Marine Engineering*, 13, 39-50 (2016).
16. Sudarsana Reddy, P and Chamkha, A.J., Soret and Dufour effects on MHD convective flow of Al_2O_3 –water and TiO_2 –water nanofluids past a stretching sheet in porous media with heat generation/absorption, *Advanced Powder Technology* 27, 1207 – 1218 (2016).
17. Raghunath and Siva Prasad, Heat and Mass Transfer on Unsteady MHD Flow of a Visco-Elastic Fluid Past an Infinite Vertical Oscillating Porous Plate: *British Journal of Mathematics & Computer Science*, ISSN: 2231-0851, Vol.: 17, Issue.: 6 (2017).